Nonlinear Dyn (2019) 95:1923–1939
https://doi.org/10.1007/s11071-018-4668-1

ORIGINAL PAPER

Nonlinear effect of biological feedback on brain attentional state

Vladimir A. Maksimenko · Alexander E. Hramov · Vadim V. Grubov · Vladimir O. Nedaivozov · Vladimir V. Makarov · Alexander N. Pisarchik

Received: 13 July 2018 / Accepted: 17 November 2018 / Published online: 26 November 2018

Abstract A nonlinear effect of biological feedback on visual perception is studied when a brain–computer interface is applied. The implemented algorithm for estimation of visual attention is based on the time–frequency analysis of human electroencephalograms in real time by measuring the amplitude of the stimulus-related brain response, which takes subsequently positive and negative values. The analysis shows that time intervals with positive amplitude are associated with periods of sustained attention, whereas time intervals with negative amplitude are related to mental fatigue. The comparison of the results obtained in two groups of subjects, one without feedback and another with feedback, demonstrate that the feedback control prolongs the periods of sustained attention. The largest interval of sustained attention in the former group reached only 100 ± 20 s versus 150 ± 40 s in the latter group. However, the mean degree of attention, estimated by averaging the brain response amplitude over the whole interval, was 27% lower in the group with feedback than in another group. The obtained results evidence that cognitive resource is limited, and therefore, to maintain high performance for prolonged time, the brain has to work in a "safe-mode" regime.

Keywords Visual attention · EEG analysis · Brain–computer interface · Biological feedback

1 Introduction

The brain neural network is a very complex nonlinear system [1,2] in which dynamics is often studied by analyzing electrical signals recorded with multichannel electroencephalography (EEG) [3]. Each EEG channel detects a total current of a large group of neurons in the neural network. The EEG signal has a complex time–frequency structure with specific dominant frequencies (δ, α, β, γ, etc.) and characteristic oscillatory patterns [4–7]. Since there is a strong correlation between electrical brain activity and brain states [8], the analyses of EEG time–frequency structure and oscillatory patterns provide information about dynamical states of the neural network.

The interest in studying brain dynamics using EEG is not limited to fundamental knowledge, but also caused by important applications, for example, in brain–computer interfaces (BCIs) which require real-time detection and analysis of electrical (or magnetic) brain activity with subsequent transformation

---

V. A. Maksimenko · A. E. Hramov · V. V. Grubov ·
V. O. Nedaivozov · V. V. Makarov · A. N. Pisarchik
REC "Artificial Intelligence Systems and Neurotechnology", Yuri Gagarin State Technical University of Saratov, Saratov, Russia 410054

A. E. Hramov (✉)
Faculty of Nonlinear Processes, Saratov State University, Saratov, Russia 410028
e-mail: hramovae@gmail.com

A. N. Pisarchik
Center for Biomedical Technology, Technical University of Madrid, Campus Montegancedo, Pozuelo de Alarcon, 28223 Madrid, Spain

of obtained information into computer commands for feedback control [9–11]. The general aim of BCI is to repair or enhance human performance [12], for example, to help paralyzed people to control prosthetic devices [13] and interact with the environment [14]. This requires a permanent information exchange between brain and computer, i.e., two-way data transfer in the BCI, where the information arriving from the brain to the computer allows continuous monitoring of the brain state evolution and generation of control commands for hardware. On the other hand, the information which comes back to the operator is used either by the operator for self-control of his/her brain activity or by hardware/software to affect the brain directly. Such exchange of information between brain and computer is known as *biological feedback*.

The biological feedback is required for different types of BCI. For instance, in neuroprosthetics, a sensory feedback allows the user to "feel" rigidity and elasticity of the object and therefore effectively modulate the grasping force of a prosthesis. As was recently shown, the feedback is an efficient tool for training people to control a prosthesis [15]. Along with visual and auditory stimuli [16], the feedback was used to stimulate median and ulnar nerves according to information provided by artificial sensors from a hand prosthesis [17]. This feedback control enabled the participant to effectively modulate the grasping force of the prosthesis without visual or auditory feedback [17]. In addition to motor-related brain activity, the feedback can be used to control psycho-physiological states, especially those associated with high mental functions. The effects of feedback control on the time–frequency EEG structure during performance of mental task were studied many years ago. For instance, De Pascalis and Silveri [18] demonstrated that biofeedback regulation and convert mental activity affect EEG α-asymmetry. Later, the influence of feedback on the performance in strategic skill acquisition tasks was also investigated [19]. Obviously, the feedback is a key part of the human–machine systems. At the same time, its effective use for controlling brain dynamics requires a deep understanding of the basic principles of neural brain activity under this type of control.

It is known that feedback control can dramatically change the behavior of a nonlinear system. For instance, the feedback can lead to a more complex or even chaotic behavior in simple systems, such as a pendulum [20,21]. Although a weak control can be achieved even with linear feedback, nonlinear feedback provides advanced control opportunities. For example, linear-plus-nonlinear feedback applied to a dynamical system can control bifurcations and the system transition to various states [22–24]. The application of nonlinear feedback was extended and generalized for a wide class of dynamical systems [25]. Furthermore, the implementation of feedback control is not limited to model systems. One can find examples of complex feedback control in many natural and engineering systems, e.g., sway reduction on container cranes [26], the plunge and pitch motions of a wing [27], lasers [28,29]. In the same way, the human brain, being a strongly nonlinear system, can also be affected by feedback in an unpredictable way. Unfortunately, the main principles of brain feedback control are not yet established.

According to this, the aim of the present work is to study how feedback control affects human attention during visual perception. This research was stimulated by recently obtained results [30] on the effect of a real-time BCI on human attention. To quantify visual attention, we developed an algorithm based on the time–frequency structure of EEG signals. As soon as the subject's attention felt, an audio signal was sent to inform his about it, and after that, his attention increased. We expected that such feedback control will also increase a mean level of attention during the whole experimental session. However, this is not true. The results of the present work show a rather unexpected outcome. Although the feedback control does enlarge time intervals with a relatively high level of attention, the mean level of attention is not so high as in the uncontrolled group.

The paper is organized as follows. In Sect. 2, we describe materials and methods, and in Sect. 3 the results of the EEG analysis. Then, in Sect. 4 we demonstrate nonlinear effects of the feedback control on the brain dynamics and provide a detailed discussion in Sect. 5. Finally, main conclusions are given in Sect. 6.

2 Materials and methods

2.1 Subjects, stimuli and recordings

Twelve healthy subjects from a group of students, researchers, and staff of the Yuri Gagarin State Technical University of Saratov, males and females, between the ages of 20 and 28 with normal or corrected-to-normal visual acuity participated in the experiment. All participants provided informed written consent before the experiment.

Our recent studies [30] provide the experimental evidence that the use of ambiguous images as visual stimuli increases subject's alertness. Therefore, in the present work all experiments were carried out with ambiguous visual stimulus, namely, with the Necker cube [31]. Among many types of bistable visual stimuli, the Necker cube is the most explored one. Due to its simplicity and symmetry, it was widely explored in many psychological and neurophysiological experiments [32–34] and theoretical models [34–36]. At the same time, detailed studies of neural mechanisms of bistable perception demonstrated similar results for other bistable stimuli (see, e.g., [37]). The important advantage of this image over the others is the possibility to control its bistability by varying the contrast of inner lines, as shown in Fig. 1. Since this cube has transparent faces and visible edges, the observer without any perceptional abnormalities perceives it as a 3D object due to the specific position of the ribs. Bistability in perception of the Necker cube consists in its interpretation as either left- or right-oriented, depending on the contrast of the inner edges. The contrast $g \in [0, 1]$ of the three edges centered in the left lower corner was used as a control parameter. At the same time, the contrast of the other three inner edges centered in the right upper corner was set to $1-g$. The values $g = 1$ and $g = 0$ correspond, respectively, to 0 (black) and 255 (white) pixels' luminance of the inner lines. Therefore, we can define a contrast parameter as $g = y/255$, where y is the brightness of the inner lines using the 8-bit grayscale palette. Along with the cases of unambiguous fully left- ($g = 0$) or fully right-oriented ($g = 1$) cubes and completely ambiguous ($g = 0.5$) cube, we presented samples with various configurations in the ranges of $0 < g < 0.5$ and $0.5 < g < 1$ corresponding to statistically left-oriented and right-oriented cubes, each differed from the previous one. Presenting the stimuli with different configuration allowed us to minimize memory effect and habituation of the subject, and considered each perception independently of the previous one. For good statistics, we analyzed many EEG trials obtained during perception of a large number of sequentially displayed images.

The subjects were comfortably sitting at a 70–80 cm distance from a 24″ LCD monitor with an approximately 0.25 rad visual angle. The Necker cubes with different contrasts of the inner edges were displayed on a white background in the middle of the monitor with a spatial resolution of 1920 × 1080 pixels and a 60-Hz refresh rate.

The perception of an ambiguous image is known to be associated with an increase in electrical activity of neurons in the occipital lobe [38,39], that is, explained by the existence of visual areas in the occipital lobe and attentional areas in parietal lobe [40]. Therefore, in the present work, we restricted our analysis to the EEG recordings from 5 electrodes only, located in the occipital (O1 and O2) and parietal (P3, P4, Pz) lobes [30] according to the 10–20 electrode layout [41], as shown in Fig. 2.

To register the EEG data, the cup adhesive Ag/AgCl electrodes were fixed on the scalp with the help of "Tien–20" paste. Before the experiment, we put the abrasive "NuPre" gel on the scalp to increase the skin conductivity. After the electrodes were installed, we monitored the impedance which varied within a 2–5-kΩ interval. The ground electrode N was located above the forehead, and the reference electrodes A_1 and A_2 were attached to the mastoids. For filtering the EEG signals, we used a band-pass filter with cut-off points at 0.016 Hz (HP) and 70 Hz (LP), as well as a 50-Hz Notch filter. We also registered the electrooculograms (EOG) to remove eye blink artifacts by means of our own method based on the Gram–Schmidt orthogonalization [42]. For amplification of the EEG and EOG signals and analog-to-digital conversion, we used the electroencephalograph "Encephalan–

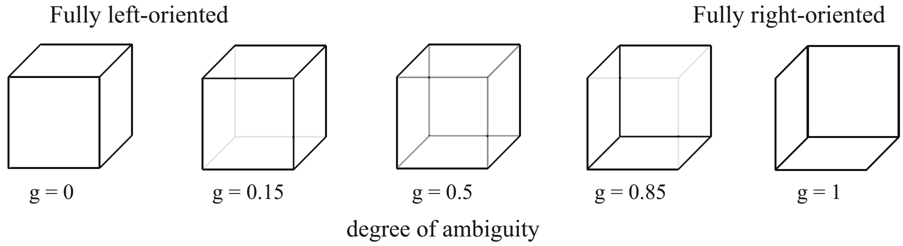

Fig. 1 Bistable visual stimuli. Examples of Necker cubes with different values of control parameter g defined by the contrast of inner lines

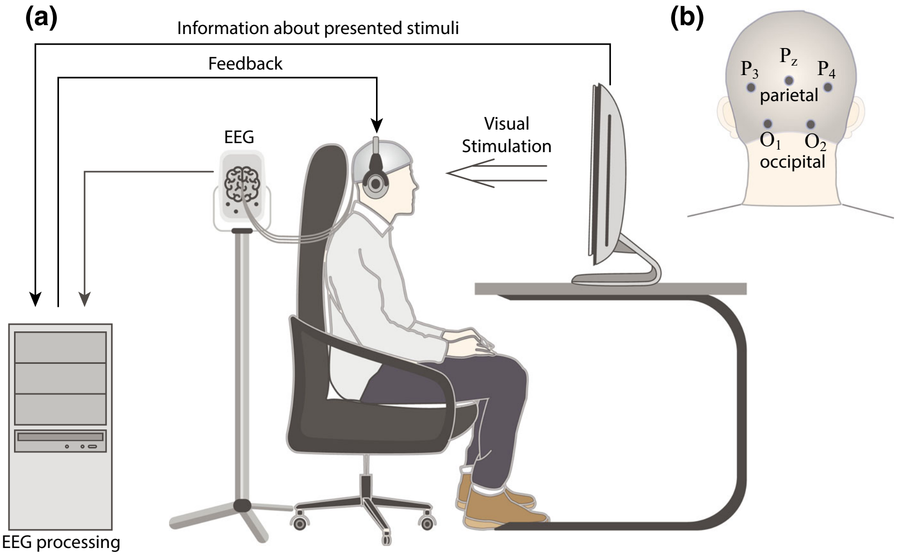

Fig. 2 Experimental design. **a** The volunteer is subjected to the visual task which includes perception and primary processing of visual information. EEG signals are recorded from parietal and occipital areas and processed in real time. The feedback is realized via audio signal. **b** Location of five recording electrodes on the scalp

EEGR–19/26" ("Medikom-MTD," Taganrog, Russia) with multiple EEG channels and two-button input device (keypad).

2.2 Experimental procedure

The experiment contained two sessions. All twelve subjects were initially divided into two groups, six in each group. In the first session, the experiments were performed in both groups without feedback control. The feedback was applied to the second group only, and only in the second session. The design of our experiment is illustrated in Fig. 2. All participants were instructed to press either left or right key on the input device depending on their first impression on the cube orientation at each presentation.

For all subjects, the second session was performed one month after the first session. Each session lasted 30 minutes. Each Necker cube was presented for a short interval between 1.0 and 2.0 s. Such a relatively short duration of the stimuli presentation was chosen to reduce the stabilization effect because, as known [43], the probability of persisting interpretation of a previous image strongly depends on the stimulus duration. For the Necker cube, the required time of consistent observation was found to be about 1.0 s [44]. Although the "memory" effect cannot be completely avoided, it can be significantly diminished by making a length of stimulus exhibition shorter than 2.0 s. Moreover, a random change in the control parameter g also prevents the perception stabilization. Lastly, to draw away the observer's attention and make the perception of the next Necker cube independent of the previous one, different abstract pictures were exhibited for about 5–6 s between subsequent demonstrations of the Necker cube images.

2.3 Algorithm for real-time EEG analysis

The algorithm flowchart is schematically illustrated in Fig. 3. It includes six steps:

1. *EEG acquisition* As mentioned above, the EEG signals were recorded by five electrodes (O_1, O_2, P_3, and P_4, P_z) with a 250-Hz sampling rate. The typical recording set is shown in Fig. 3a. The starting time of the ith image presentation is shown by a vertical dashed line in the right panel.
2. *Time–frequency EEG analysis* We used the continuous wavelet transform [45]. The wavelet energy spectrum $E^n(f,t) = \sqrt{W_n(f,t)^2}$ was calculated for each EEG channel $X_n(t)$ in the frequency range of $f \in [1, 30]$ Hz. Here, $W_n(f,t)$ is the complex-valued wavelet coefficients calculated as

$$W_n(f,t) = \sqrt{f} \int_{t-4/f}^{t+4/f} X_n(t)\psi^*(f,t)\mathrm{d}t, \qquad (1)$$

where $n = 1, \ldots, N$ is the EEG channel number ($N = 5$ being the total number of channels

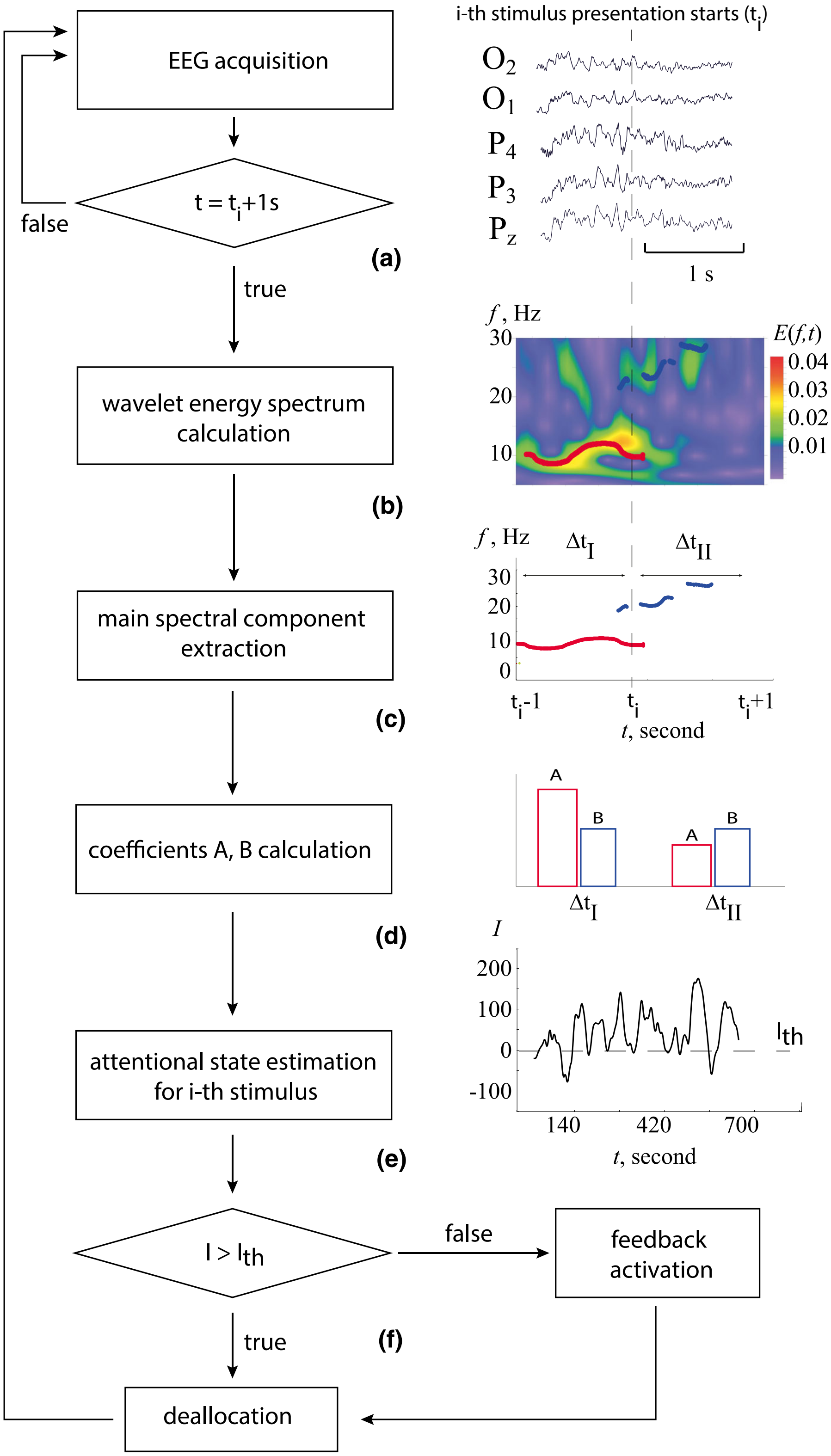

Fig. 3 Algorithm flowchart. **a** EEG acquisition and a typical set of EEG recordings from five channels (t_i is the starting time of ith presentation). **b** Wavelet energy spectrum calculation and typical fragment of wavelet energy distribution during perception of ith stimulus. **c** Extracting spectral components and typical time dependence of main spectral components during the transition from background EEG (Δt_I) to the perception of the visual stimulus (Δt_{II}). Red and blue colors indicate α (red) and β (blue) frequency bands, respectively. **d** Histogram showing the values of A and B calculated by Eqs. (3) and (4) in time intervals Δt_I and Δt_{II}. **e** Temporal evolution of the degree of visual attention I during experimental session. The threshold value $I_{\mathrm{th}} = 0$ is shown by the horizontal dashed line. **f** Logical condition for feedback control activation

used for the analysis) and “*” defines the complex conjugation.

The important problem in using the wavelet transform is a choice of the appropriate mother wavelet for data analysis. This choice depends on both the aim of the study and characteristics of the analyzed signal. The most commonly used mother wavelets are Morlet, MHAT (or DOG), Paul, and FHAT. Two of these mother wavelets, MHAT and FHAT, are real, while the others are complex [46]. In this work, we used the wavelet analysis for the extraction of the main spectral component with respect to the phase of the brain rhythm. Therefore, possible options for the mother wavelet in this particular study are mostly reduced to complex wavelets. According to Ogden et al. [47], the complex Morlet wavelet is very convenient for the analysis of multiple-frequency non-stationary signals, such as EEG recordings which consist of a great number of rhythms and oscillatory patterns. The comparison of the results on the EEG wavelet analysis with different complex mother wavelets [46] shows that the complex Morlet wavelet provides clearer wavelet surface and better overall resolution in the time–frequency domain. This feature allows localizing (with good enough accuracy) time moments when the signal structure is altered, that is, very useful for the main spectral component extraction.

The Morlet mother wavelet function $\psi(f,t)$ is defined as

$$\psi(f,t) = \sqrt{f}\pi^{1/4} \mathrm{e}^{j\omega_0 f(t-t_0)} \mathrm{e}^{f(t-t_0)^2/2}, \qquad (2)$$

where $\omega_0 = 2\pi$ is the central frequency of the Morlet mother wavelet [48]. Figure 3b illustrates typical time–frequency dynamics of the wavelet spectral energy value $E(f,t)$ during visual perception. One can see that time–frequency structure of the EEG signals is characterized by a local increase in the wavelet energy value in the α-frequency range (8–12 Hz) before image presentation and in the β-frequency band (15–30 Hz) during image perception.

3. *Extracting spectral components* In order to describe changes in the time–frequency structure of the EEG signals, induced by presented visual stimuli, we analyzed dynamics of the main spectral components. We defined the main component as a frequency at which the wavelet energy exhibits a local maximum in the power spectrum. First, in the energy spectrum $E(f)$ we found frequencies corresponding to all local maxima. Then, for each channel we took into account up to five spectral components $(f_1, \dots, f_5)$ at which global (at f_1) and four local maxima were observed with corresponding wavelet energies $E(f_1), \dots, E(f_5)$, where $E(f_1) > E(f_2) > \cdots > E(f_5)$. Then, having calculated the wavelet spectrum $E(f)$ and extracted the frequencies $(f_1, \dots, f_5)$ for subsequent times, we analyzed how the main spectral components evolved in time.

   According to our recent work [30], visual attention is associated with the interplay between α (8–12 Hz) and β (15–30 Hz) frequency bands in occipital and parietal areas. Therefore, we considered the values $(f_1, \dots, f_5)$ belonging to these particular frequency bands. Figure 3c shows a typical time dependence of the frequencies $(f_1, \dots, f_5)$ belonging to α and β frequency bands, during the transition from background EEG (Δt_I) to the perception of visual stimulus (Δt_{II}). Red and blue colors indicate the belonging of the spectral component to either α or β frequency band.

4. *Quantification of perceptual process* In order to quantify the efficiency of the stimulus processing by the observer, we compared brain dynamics in 1-s intervals immediately before and after the onset of stimulus presentation. For this purpose, we calculated the location of the maximal spectral components during the presentation of ith stimulus $(A_i^1, A_i^2, B_i^1, B_i^2)$. These values statistically describe the dominant frequencies using EEG data taken from all occipital and parietal channels before and after the onset of image presentation, as follows

$$A_i^{1,2} = \sum_{n=1}^{N} \int_{t \in \Delta t^i_{1,2}} \left[\sum_{k=1}^{K} \xi_k^n(t') \mathrm{d}t' \right],$$
$$\xi^n(t) = \begin{cases} 1/k, & \text{if} \quad f_k^n \in \Delta f_\alpha, \\ 0, & \text{if} \quad f_k^n \notin \Delta f_\alpha. \end{cases} \qquad (3)$$

$$B_i^{1,2} = \sum_{n=1}^{N} \int_{t \in \Delta t^i_{1,2}} \left[\sum_{k=1}^{K} \xi_k^n(t') \mathrm{d}t' \right],$$
$$\xi^n(t) = \begin{cases} 1/k, & \text{if} \quad f_k^n \in \Delta f_\beta, \\ 0, & \text{if} \quad f_k^n \notin \Delta f_\beta. \end{cases} \qquad (4)$$

Here, $N = 5$ is the total number of EEG channels taken into consideration, f_k^n is the location of kth maximal spectral component belonging to nth channel, $K = 5$ is the number of analyzed spectral components, and $\Delta t_{1,2}^i$ indicate 1-s time intervals preceding and following the ith image presentation (see Fig. 3c). The histogram in Fig. 3d shows typical A and B values calculated for each image presentation.

5. *Assessment of subject's attention.* According to existing works on human attention, including our recent papers [30,49], visual attention is associated with activation of an "attentional center" in the parietal cortex, which operates in the 15–30 Hz range [40], i.e., increasing visual attention activates β-waves in the parietal area. In addition, visual stimulus processing strengthens connectivity between occipital and parietal areas in α- and β-frequency bands [50,51], which, in turn, causes a growth of β-activity in the occipital cortex. Finally, many studies evidence that visual information processing along with an increase in β-activity simultaneously inhibits α-wave activity. According to our recent study [49], the increased visual attention causes a percept-related increase in β-activity with an accompanying decrease in α-activity.
   Taking into account the above observation, the subject's attention during visual stimulus processing can be quantified as
   $$I(t_i) = \frac{(\overline{A}_i^1 - \overline{A}_i^2) + (\overline{B}_i^2 - \overline{B}_i^1)}{2}, \qquad (5)$$
   where $\overline{A}_i^{1,2}$ and $\overline{B}_i^{1,2}$ define the values of $A_i^{1,2}$ and $B_i^{1,2}$ averaged over six preceding events ($i - 6, \ldots, i$). Such averaging is performed in accordance with our previous results [30], where we demonstrated that when stimuli are processed during a short time, the subject sometimes exhibits low attention during a single event, even while demonstrating overall high attention during the whole session. One can see that $I(t_i)$ reaches a maximal positive value, if the terms in both brackets in Eq. (5) are high and positive. This corresponds to a state of high attention when $\overline{A}_i^1 > \overline{A}_i^2$ and $\overline{B}_i^2 > \overline{B}_i^1$, i.e., when α-activity decreases and β-activity increases. On the contrary, $I(i)$ reaches a minimal negative value when $\overline{A}_i^1 < \overline{A}_i^2$ and $\overline{B}_i^2 < \overline{B}_i^1$. Finally, $I(i)$ is zero when changes in α- and β-activity are insignificant.
   Figure 3e shows typical evolution of attention $I(t)$ during the experimental session.
6. *Feedback activation.* The value of attention I was calculated using Eq. (5) after each visual stimulus was processed by the subject, and compared to the threshold value I_{th} (see Fig. 3f). In our study, I_{th} was set to zero, and the feedback was organized as a short audio tone after the stimulus was processed, each time when $I \leq I_{\text{th}}$. The subject was previously instructed to associate this sound message with a low attention state.

3 Results of EEG analysis

At the first stage, we analyzed the effect of the feedback control on subject's cognitive performance by comparing I values obtained in the first and second sessions. Figure 4a shows a typical change in the attention degree I for one subject from the first group (without feedback) during the first (red line) and second (blue line) experimental sessions. One can see that the attention degree I oscillates with average period of $T \approx 150$ s. During each period, the subject processes about 20 visual stimuli. We suppose that time intervals where $I > 0$ are associated with the state of increased attention, when a large group of neurons actively participate in visual information processing, whereas the intervals where $I < 0$ are related to a refractory state of neural dynamics.

We compared the mean values of attention during the first ($\overline{I}_I$) and second ($\overline{I}_{II}$) experimental sessions for every subject from the first (GROUP1; without feedback) and second (GROUP2; with feedback) groups to find the difference $\Delta I = \overline{I}_{II} - \overline{I}_I$. As seen from Fig. 4b, the mean difference between $\overline{I}_I$ and $\overline{I}_{II}$ in GROUP2 is positive ($\overline{\Delta I} > 0$), while in GROUP1 it is negative ($\overline{\Delta I} < 0$), in spite of a relatively large standard deviation (SD) among different subjects in the group. In order to define, whether or not the change between $\overline{I}_I$ and $\overline{I}_{II}$ is significant for these groups, we applied the Wilcoxon signed-rank test, usually used to compare two related short samples. As a result, we obtained $p = 0.345$ and $p = 0.51$ for the first and second group, respectively. This evidences that the changes in the mean level of visual attention between the first

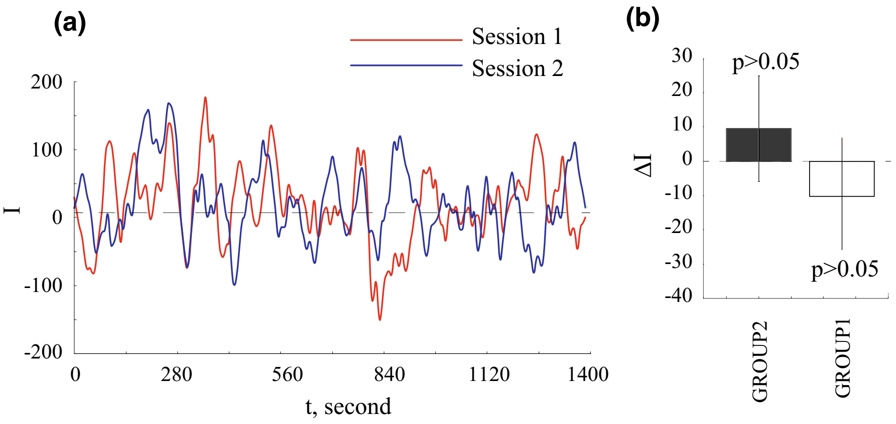

Fig. 4 Results of feedback control. **a** Typical time evolution of the degree of visual attention I during first (red) and second (blue) experimental sessions for one subject from the first group (without feedback). **b** Changes in the mean value of attention I during the first and second sessions for subjects from the first (white box, without feedback) and second (black box, with feedback) groups. The data are shown as mean ± SD ($*p < 0.05$ by Wilcoxon signed-rank test, $n = 6$)

and second sessions in both groups are insignificant. For the group without feedback control, this result was expected because the subjects demonstrated more or less the same mean value of I in two different sessions, and for the controlled group, it is rather surprising. The reason for this kind of behavior can be understood if we suppose that the cognitive resource to maintain sustained attention for a long time is limited, so that the brain needs rest to recover its cognitive resource.

For deeper understanding of the feedback control effect on the percept-related brain activity, we analyzed the dependency of I in detail. More precisely, for each experimental session, we extracted time intervals where $I > 0$. Such intervals marked by δ_1, δ_2 and δ_3 are shown in Fig. 5. The values of $\delta_{1,2,3}$ define the lengths of these intervals. As already mentioned above, we suppose that positive values of the brain response amplitude indicate increased attention of the subject and the brain ability to allocate its cognitive resource for visual information processing. On the other hand, time intervals with negative I correspond to a recovery period of the parieto-occipital neural network and redistribution of mental workload over more complex neural network.

For every interval δ_i, we calculated coefficient $\gamma(\delta)$ associated with the mean degree of attention over interval δ_i of sustained attention, as follows

$$\gamma(\delta) = \int_{t' \in \delta_i} I(t')\mathrm{d}t'. \qquad (6)$$

As a result, for each session we obtained a set of values $(\delta, \gamma(\delta))$ which characterized the intervals, during which the subject demonstrated high degree of attention.

In Fig. 6, we plot the attention state of every subject in the two-parameter space of $(\delta, \gamma(\delta))$ from the first (without feedback) (Fig. 6a) and second (with feedback) (Fig. 6b) groups. The red and blue dots indicate the values obtained during the first and second experimental sessions, respectively. We remind that in the first session in both groups, the feedback control was not applied. It was only applied in the second session in GROUP2 (blue dots in Fig. 6b). One can see that in GROUP1 there is no difference between the distributions obtained in two sessions, whereas in GROUP2 the difference is significant. In the first session (without feedback) in GROUP2, all (red) points are distributed in the range of $\delta < 100$ s, and in the second session (with feedback), some (blue) points lie in the region with $\delta > 100$ s and $\gamma < 100$. This means that the feedback control forces the subject to maintain his/her attention on the visual stimuli for longer time than in the first session (without feedback).

Since the cognitive brain resource is limited, the occurrence of prolonged intervals of sustained attention leads to a decrease in the mean value of attention I calculated for these intervals, as clearly seen from Fig. 6a, b. In GROUP1, the subjects sometimes exhibit high mean values of attention ($\gamma(\delta) > 100$) in both

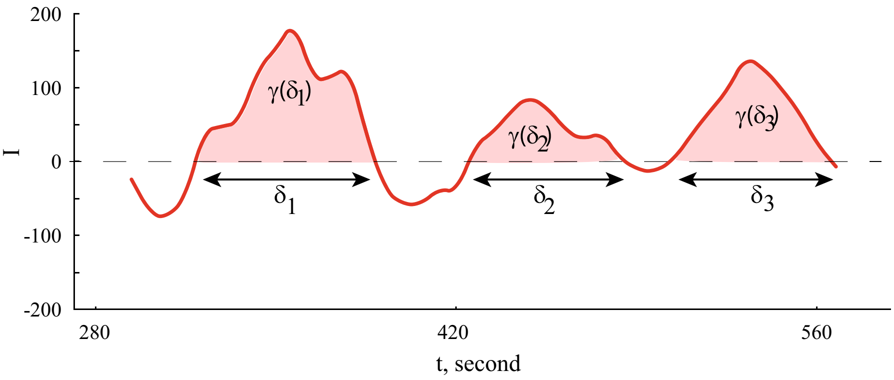

Fig. 5 Solid red curve shows typical fluctuations of stimulus-related brain response amplitude I. $\delta_{1,2,3}$ define the length of time intervals, for which the brain response amplitude is positive ($I > 0$) (time intervals with sustained attention). $\gamma(\delta_{1,2,3})$ are the mean values of the brain response amplitude over these intervals, calculated with Eq. (6)

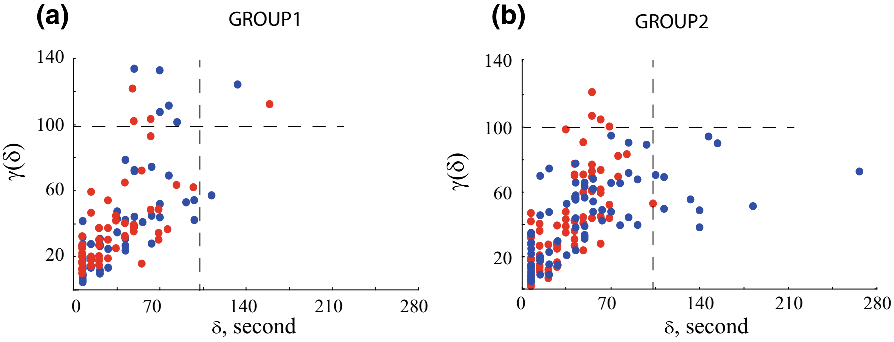

Fig. 6 Set of values $(\delta,\gamma(\delta))$, which characterize the intervals, during which the subject demonstrated high degree of attention, calculated for first (red) and second (blue) sessions for subjects from **a** control and **b** experimental groups. δ defines interval length, $\gamma(\delta)$ reflects mean degree of attention (6) during this interval

sessions (Fig. 6a), and in GROUP2, the subjects have high mean values of attention ($\gamma(\delta) > 100$) in the first session only (i.e., without feedback), but not in the second session (with feedback) (Fig. 6b). Nevertheless, the number of time intervals where the mean attention degree takes a positive value ($\gamma(\delta) > 0$) is higher in GROUP2 than in GROUP1. This means that the feedback control increases not only the duration of time intervals of sustained attention, but also the number of these intervals.

Finally, in order to statistically characterize the changes in the values δ and $\gamma(\delta)$, we found their maximal values $\delta^{\max}_{I,II}$ and $\gamma^{\max}_{I,II}$ obtained during the first and second sessions in two groups. Then, we calculated the ratios of these maxima, i.e., $\gamma^{\max}_{II}/\gamma^{\max}_{I}$ and $\delta^{\max}_{II}/\delta^{\max}_{I}$. The obtained results are summarized in Table 1 for GROUP1 and Table 2 for GROUP2. The mean ratios $\gamma^{\max}_{II}/\gamma^{\max}_{I}$ and $\delta^{\max}_{II}/\delta^{\max}_{I}$ are presented in Fig. 7 as mean±SD for subjects from GROUP1 (white box) and GROUP2 (black box). One can see that the ratio $\delta^{\max}_{II}/\delta^{\max}_{I}$ for the subjects from GROUP2 is higher than for GROUP1 (1.6±0.59 versus 1.14±0.59; see Fig. 7a). This evidences that the feedback control increases the maximum duration of the state of sustained attention. The statistical analysis of the values $\delta^{\max}_{I,II}$ obtained in the first and second sessions performed via Wilcoxon signed-rank test yielded $p < 0.05$ for GROUP2 and $p = 0.893$ for GROUP1.

While the maximum duration of the time interval of sustained attention ($I > 0$) increases in the presence of feedback, the maximum mean value of I (within this interval) decreases. This weakening of attention is demonstrated in Fig. 7b through the ratio $\gamma^{\max}_{II}/\gamma^{\max}_{I}$. One can see that the ratio $\gamma^{\max}_{II}/\gamma^{\max}_{I}$ is equal to 0.71 ± 0.08 and 1.12 ± 0.56 for GROUP2 (with feedback) and GROUP1 (without feedback), respectively. The Wilcoxon signed-rank test provided $p < 0.05$ for GROUP2 and $p = 0.686$ for GROUP1.

4 Effect of feedback control

Perception and processing of visual stimulus are known to induce stimulus-related brain response in the parieto-occipital part of the brain [40]. This response is caused by the excitation of neuronal activity in attentional and visual centers and can be measured as changes in the energy of α and β-waves. The amplitude of this response can be measured by terms of α- and β-wave.

Table 1 The values of $\delta_{I,II}^{\max}$ and $\gamma_{I,II}^{\max}$ calculated for GROUP1 during sessions 1 and 2

Subject	$\gamma^{\max}$			$\delta^{\max}$ (s)		
	Session 1 ($\gamma_I^{\max}$)	Session 2 ($\gamma_{II}^{\max}$)	Ratio ($\gamma_{II}^{\max}/\gamma_I^{\max}$)	Session 1 ($\delta_I^{\max}$)	Session 2 ($\delta_{II}^{\max}$)	Ratio ($\gamma_{II}^{\max}/\gamma_I^{\max}$)
1	100	113	1.13	16	19	1.18
2	104	84	0.8	49	11	0.22
3	161	110	0.68	32	60	1.87
4	42	94	2.23	6	10	1.67
5	85	71	0.83	41	32	0.78
6	103	111	1.07	15	17	1.13
Mean (± SD)	99.16 (±38.29)	97.16 (±17.17)	1.12 (±0.56)	28.8 (±16.78)	24.83 (±18.94)	1.14 (±0.59)

$\delta_{I,II}^{\max}$ are maximum lengths of time intervals during which the subject maintained sustained attention ($I > 0$). $\gamma_{I,II}^{\max}$ are maximum values of the mean brain response amplitude

Table 2 The values of $\delta_{I,II}^{\max}$ and $\gamma_{I,II}^{\max}$, calculated for GROUP2 during sessions 1 and 2

Subject	$\gamma^{\max}$			$\delta^{\max}$ (s)		
	Session 1 ($\gamma_I^{\max}$)	Session 2 ($\gamma_{II}^{\max}$)	Ratio ($\gamma_{II}^{\max}/\gamma_I^{\max}$)	Session 1 ($\delta_I^{\max}$)	Session 2 ($\delta_{II}^{\max}$)	Ratio ($\gamma_{II}^{\max}/\gamma_I^{\max}$)
1	121	94	0.77	14	38	2.71
2	104	78	0.75	16	19	1.18
3	107	89	0.83	24	29	1.2
4	68	42	0.61	6	11	1.83
5	100	62	0.62	16	20	1.25
6	97	69	0.71	37	53	1.43
Mean (±SD)	99.5 (±17.53)	72.33* (±19.06)	0.71 (±0.08)	18.83 (±10.59)	28.33* (±15.22)	1.60 (±0.59)

$\delta_{I,II}^{\max}$ are maximum lengths of time intervals during which the subject maintained sustained attention ($I > 0$). $\gamma_{I,II}^{\max}$ are maximum values of the mean brain response amplitude

*$p < 0.05$ by Wilcoxon signed-rank test, $n = 6$

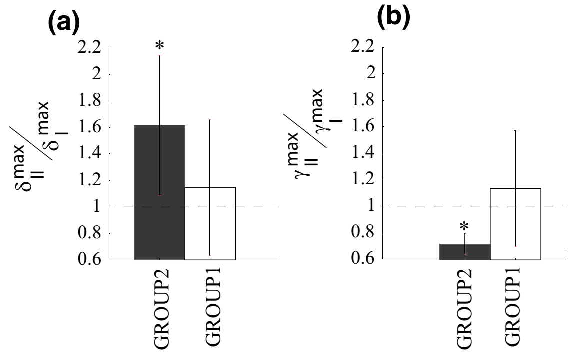

Fig. 7 Ratio between values **a** $\delta_I^{\max}$ and $\delta_{II}^{\max}$ and **b** $\gamma_I^{\max}$ and $\gamma_{II}^{\max}$ obtained for the first and second sessions for subjects from GROUP1 (white boxes) and GROUP2 (black boxes). The data are shown as mean±SD (*$p < 0.05$ by Wilcoxon signed-rank test, $n = 6$)

Also, the task complexity is known [30] to increase the mean energy by engaging more neurons for stimuli processing. This means that the brain increases its power by enlarging a size of the neural network involved in information processing in order to solve more difficult cognitive task. If the mean brain response amplitude is defined as I and the mental workload level as M, then the function $I(M)$ monotonically increases when $M < M*$, where M^* is a critical workload.

On the other hand, during valuation of a prolonged visual task, the mental fatigue affects brain activity, i.e., the mean brain response amplitude decreases during fatigue-inducing mental tasks [52]. Therefore, if the mean brain response amplitude is defined as I and T being the time which the brain spends for solving the task, then $I(T)$ monotonically decreases when $T >$

T^*, where T^* is a time interval for which the effect of mental fatigue is not pronounced.

Taking the foregoing into account, we suppose that the feedback which informs the subject that his/her brain response amplitude decreases makes the brain to increase again its processing power and therefore the mean brain response amplitude. Thus, the feedback realized with BCI leads to higher I during the prolonged session, as compared to the amplitude obtained for session without BCI.

At the same time, we found that the value of I obtained during the first (feedback-controlled) sessions remained the same as for the session without feedback. Figure 8 illustrates a typical time evolution of the brain response amplitude. $I(t)$ exhibits fluctuations which contain traces with positive and negative I corresponding to high brain activity and refractory periods of neural ensemble activity, respectively. Let us now consider the time interval $T^1 < DeltaT < T^2$ where the neuronal ensemble is involved in generation of the percept-related brain response. Having compared the $I(t)$ dependence during Session 1 (without feedback) and Session 2 (with feedback), one can see that in the former case (Fig. 8a) the brain response amplitude exhibits the higher peak and reaches the maximum value faster than in the latter case (Fig. 8b). At the same time, the duration of the interval with positive I is larger in the latter case ($\Delta T_{II} > \Delta T_I$). The process is subsequently repeated many times during each session, and the comparative results are averaged over whole session time.

Thus, the nonlinear effect of biological feedback on the brain attentional state can be summarized as follows. Although the feedback decreases a maximum value of the brain response, it activates a nonlinear mechanism which suppresses neural excitation to maintain the brain activity at a relatively high level during larger time.

5 Discussion

The obtained results evidence the following nonlinear effects.

(i) The degree of attention (DA) estimated on the base of spectral properties of parieto-occipital EEG evolves in time according to a periodic law. The time intervals during which DA is high are replaced with ones with lower DA.

(ii) Biological feedback implemented via a sound message which informs the subject about decreasing DA leads to an increase in the duration of intervals with high DA, but does not affect the mean DA during the session.

The comparison of our results with recent works of other authors allows us to suppose that in the absence of biological feedback the features of the brain activity during a prolonged mental task are affected by two main neural mechanisms. The first one, known as mental fatigue, consists in the brain inability to complete the mental task which requires a high level of sustained attention in the absence of discernible cognitive failure [53]. According to Mizuno et al. [54], mental fatigue affects brain activity of healthy subjects during accomplishing fatigue-inducing mental tasks, including a prolonged visual stimulus. The effect of mental fatigue was also demonstrated in terms of behavioral performances. In particular, Bonnefond et al. [55] showed that the behavioral performance in the accuracy and speed declines in time. Furthermore, Boksem et al. [56] found that when the duration of the experiment is increased, the number of missed and false alarms also increases, while the response speed decreases. In addition, Kato et al. [57] observed a significant increase in the reaction time and the number of errors, when the time spent for task evaluation enlarges.

Along with these behavioral signs, the effect of mental fatigue on visual attention can be estimated based on the EEG structure. For instance, Faber et al. [58] concluded that visual attention is affected by mental fatigue in the form of a decrease in the ability to suppress irrelevant information. The authors demonstrated fatigue-related signs in electrical brain activity in parieto-occipital areas by analyzing event-related potentials (ERP). Guo et al. [59] also used ERP for the analysis of the effect of mental fatigue on sustained visual attention under a long-standing monotonous task.

In the particular case of visual perception, when incoming visual information stimulates visual and attention centers across the neural network in the parieto-occipital area, the time–frequency EEG structure exhibits a stimulus-related increase in β-activity (15–30 Hz) [40] accompanied by a decrease in α-activity (8–12 Hz) across parietal and occipital regions. When β-rhythm increases and α-rhythm simultaneously decreases, we deal with a percept-related response of the parieto-occipital brain network. The

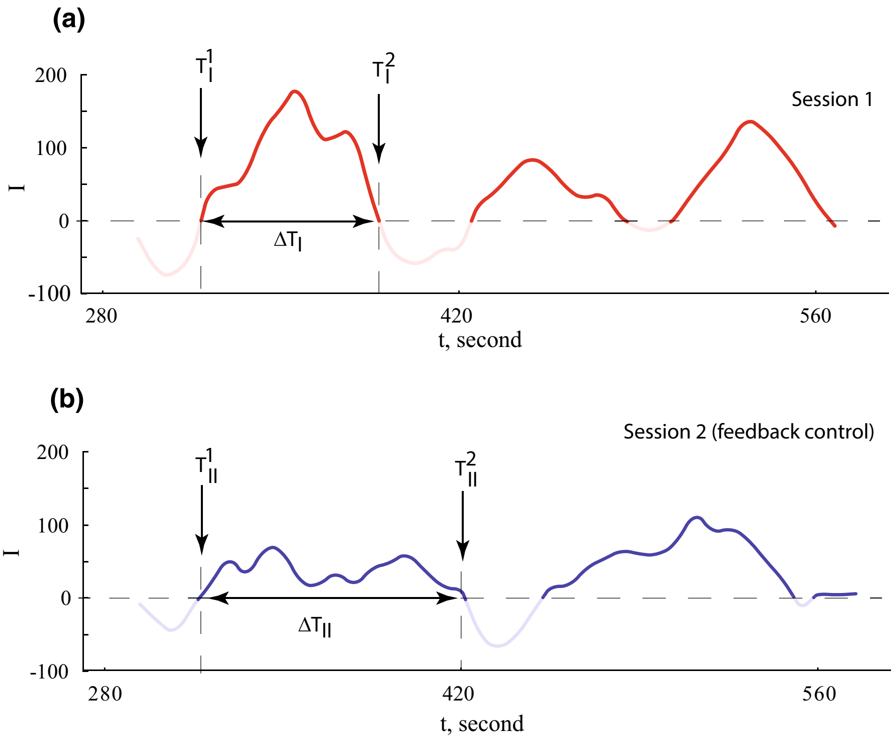

Fig. 8 Typical fragments of $I(t)$ dependency during **a** first (without feedback) and **b** second (with feedback) experimental sessions. The solid lines (above zero) show the traces of high brain response, while the transparent lines (below zero) show the refractory intervals of neural ensemble activity

amplitude of this response or the degree of attention (DA) in every time moment is measured using Eq. (5). According to Klimesch [60] and more recent work of Roy et al. [52], mental fatigue produces an increase in the energy at low frequencies ($<$ 12 Hz), including α-rhythm, accompanied by a decrease in the energy at high frequencies ($>$ 12 Hz), including β-rhythm. A decrease in the β-rhythm power density in parietal area during fatigue-inducing mental task sessions was also reported by Tanaka et al. [61] and Zhao et al. [62]. These observations physiologically justify that mental fatigue reduces human attention, i.e., DA decreases. This can be estimated by our algorithm through Eqs. (3)–(5) based on the α- and β-wave energies.

The origin of the above effect may lie in the brain ability to change a structure of the functional neural network under increasing cognitive demand. This follows from the global workspace theory (GWT), which implies that conscious perception requires coherent activity of multiple distributed brain regions [63]. According to GWT, the tasks which can effortlessly be performed activate a limited number of neurons in the brain network. Conversely, cognitive tasks which require sustained attention engage a set of long-distance connections coordinating the activity of multiple distributed brain regions [64]. In the recent paper of Finc et al. [65], the authors studied changes in the whole-brain functional network under increasing cognitive demands of working memory, based on the network approach. They demonstrated that an increase in cognitive demand results in a decrease in modularity of the whole-brain neural network. This in turn implies a less segregated and more integrated network connectivity patterns. With these results in mind, Guo et al. [66] showed that such brain network reorganization can also be induced by a periodic visual stimulation. Having analyzed the steady-state visual potential (SSVEP), the authors demonstrated that the main sources of SSVEP are located in parieto-occipital and frontal areas and connections between these areas increase during stimulation. In our previous experiments on perception and preliminary processing of visual stimulus, we also observed increasing connectivity between neural structures in parietal and occipital areas [49]. Such increasing connectivity was shown to be positively related to a change in the amplitude of the stimulus-related brain response in parietal and occipital areas. According to GWT [65], high cognitive demand due to a prolonged monotonous visual task causes an increase in connectivity between parietal and frontal areas, accompanied by a decrease in the coupling strength between neural structures in parieto-occipital area. This in turn leads to a decrease in the stimulus-related brain response amplitude and hence in DA according to Eqs. (3)–(5).

Thus, one can suppose that when cognitive demand is increased, the interplay between the processes of mental fatigue and brain network reorganization forms an oscillatory mode of the brain dynamics. The periodical modulation of the brain activity level was analyzed by Fox et al. [67], who considered spontaneous fluctuations of the functional MRI blood oxygen level-dependent signal. The authors demonstrated the coexistence of two groups of diametrically opposed, widely distributed brain networks on the basis of correlation (and anticorrelation) between oscillations of fMRI signals produced by them. The first group consists of brain regions routinely exhibiting task-related activations, while the second group includes regions routinely exhibiting task-related deactivation. These groups are known as task-positive and task-negative regions, respectively.

According to Ref. [68], during the accomplishing of attention-demanding cognitive tasks, the task-positive region which includes a set of frontal and parietal cortical regions routinely exhibits an increase in activity, whereas the task-negative regions, including posterior cingulate, medial and lateral parietal, and medial prefrontal cortex, routinely exhibit a decrease in activity [69,70]. When the attentional demand of the task is increased, activity in task-positive regions further increases, while activity in task-negative regions decreases. With this in mind, one can suppose that the oscillatory mode of DA (see Fig. 4) can be associated with excitation of a task-positive response in parietal cortical regions. At the same time, as was demonstrated by Fox et al. [67], the period of these oscillations varied from 60 to 100 s during the resting state, while in our study, the period of these oscillations varied up to 150 s. Such an increase can be caused by the enlargement of the size of neural ensemble (this is also evidenced by the activity increase in these regions). It can be further supposed that in the case of biological feedback the size of the neural ensemble in parietal area exhibits a further increase in order to process visual information for a prolonged time. An increase in the neuronal ensemble size leads to an increase in its excitation time, which is reflected in an increase in the period of DA oscillations. At the same time, an increase in the time intervals with high DA is accompanied by increased alternating intervals with low DA, which correspond to the refractory periods of neural ensemble activity. As a result, the mean DA does not further increase.

Such brain response to the feedback control represents a scenario by which the brain activity follows during a prolonged visual perception task in order to resist mental fatigue. It includes the distribution of the neural activity among different brain areas and the creation of long-distance connections coordinating the activity of multiple distributed area regions when the cognitive demand is increased, as follows from the global workspace theory.

Having considered brain dynamics under the effect of increasing mental workload, one has to take into account the limited brain resource. According to the review of Marois and Ivanoff [71], there are three major bottlenecks which can cause the limitation of brain ability to consciously perceive and process information. They are attentional blinks, visual short-term memory, and psychological refractory period phenomena. It is supposed that the capacity limit of a visual short-term memory storage is localized in the posterior parietal and occipital cortex and affects a structure of electrical neural activity [72] and FMR signals [73] recorded in this brain area. According to ERP [74] and FMRI [75] analyses, the neural locus of the capacity-limited process underlying the attentional blink is in the fronto-parietal network.

In this context, biological feedback is aimed to increase the capacity limit of information processing in the brain. At the same time, according to our results, the capacity enhancement cannot be achieved during a single feedback control session. In order to increase the stimulus-related brain response amplitude, the functional structure of brain network must be adjusted to process more complex workload. According to the recent review of Taya et al. [76], this can be done using cognitive training which demonstrates a high efficiency in behavioral performances [77,78]. At the same time, besides the improving behavioral performance, the authors of many papers highlight that cognitive training also affects the brain activation [79]. In particular, it was shown that the training cannot increase the brain activity very fast; the result becomes notable in the areas related to mental task evaluation only after several weeks of training [80]. In addition to the training-induced changes in the brain activity, morphological changes can also be induced by cognitive training in the adult brain [81]. Several scientists examined the effects of training on the brain structure. They found that modulations of neural structures and brain functions can occur for a relatively short period of time. Even seven-day training already induces changes in gray matter density [82]. However, six-week training induces changes in both white and the gray matters [83]. Moreover, training was shown to increase structural integrity of the brain areas [84].

To summarize, the limited capacity of information processing in the brain is attributed to peculiarities of neural dynamics and biological properties. This leads to mental fatigue which affects neural dynamics during accomplishing a monotonous task for a long time without a break. In order to address this increasing workload, the brain starts to reconfigure a functional network structure and reconstruct different neuronal subnetworks located in remote brain regions, which start to interact more intensively. This process is accompanied by the formation of task-positive and task-negative neuronal structures. The interaction between these structures causes an oscillatory mode of neuronal activity. The increasing cognitive demand results in an increase in the amplitude and the period of these oscillations due to the enlarging size of neural ensembles involved in information processing. In this paradigm, the brain ability in increasing intensity of the task-related neural response is limited by the size of neural ensemble in a particular brain area. According to this, the application of biological feedback to enhance brain ability does not result in an increase in the neural response amplitude within a single session. At the same time, such an increase is achieved after several training sessions, since the training causes morphological changes, e.g., increasing gray matter volume and structural integrity in task-related brain areas.

6 Conclusion

Human brain is a complex system which demonstrates a variety of different nonlinear phenomena, including different types of synchronous regimes [85], intermittency [86], and extreme events [87,88]. Along with nonlinear phenomena arising inside the brain, recent studies report on the regimes of brain-to-brain synchronization [89]. In all these applications, the feedback plays an important role in brain dynamics. The feedback is required for the development of brain–computer interfaces, and on the other hand, the feedback brain control is of great interest for fundamental research and different applications.

In this paper, we have described new nonlinear phenomena in the neural brain network subjected to feedback control. In particular, we analyzed the effect of feedback on neural dynamics in the parieto-occipital human cortex during perceptual processes. First, we implemented a new algorithm for estimation of the degree of visual attention in real time based on the methods of time–frequency and statistical signal analyses. Having compared the dynamics in the groups with feedback and without feedback, we found that the feedback led to an increase in time intervals during which the subject maintained a high level of sustained attention (100 ± 20 s without feedback versus 150 ± 40 s with feedback). At the same time, the degree of attention during these time intervals was 27% lower in the group with feedback than in the group without feedback. The obtained results evidence that the brain cognitive resource is limited, and therefore, when high performance is required for a long time, it switches to a "safe-mode" regime.

We believe that the results of this work can be useful for the development of brain–computer interfaces to control human mental processes.

Acknowledgements This work has been supported by the Russian Science Foundation (Grant 17-72-30003) in the part of experimental studies and intelligent control system realization for BCI. V.A.M. thanks President Program (project MK-992.2018.2) for personal support in the part of biological feedback influence analysis. A.N.P. acknowledges support from the Spanish Ministry of Economy and Competitiveness (project SAF2016-80240) in the part of neurophysiological experimental design preparation.

Compliance with ethical standard

Human participants Subjects participated in the experiment on a voluntary and gratuitous basis. All participants signed an informed medical consent to participate in the experimental work and received all necessary explanations about the process, including their agreement for further publication of the results. Acquired experimental data were processed with respect the confidentiality and anonymity of research respondents. The experimental studies were performed in accordance with the Declaration of Helsinki and approved by the local research Ethics Committee of the Yuri Gagarin State Technical University of Saratov.

Conflict of interest The authors declare that they have no conflict of interest.

References

1. Buzsaki, G., Draguhn, A.: Neuronal oscillations in cortical networks. Science **304**, 1926–1929 (2004)
2. Maksimenko, V.A., Pavlov, A., Runnova, A.E., Nedaivozov, V., Grubov, V., Koronovskii, A.A., Pchelintseva, S.V., Pitsik, E., Pisarchik, A.N., Hramov, A.E.: Nonlinear analysis of brain activity, associated with motor action and motor imaginary in untrained subjects. Nonlinear Dyn. **91**(4), 2803–2817 (2018)
3. Lopes da Silva, F.H., Nunez, P.L., Srinivasan, K.: Electric Fields of the Brain: The Neurophysics of EEG. Oxford University Press, Oxford (2006)
4. Luders, H., Noachtar, S.: Atlas and Classification of Electroencephalography. WB Saunders Co., Philadelphia (2000)
5. Guirao, J.L.G., Luo, A.C.J.: New trends in nonlinear dynamics and chaoticity. Nonlinear Dyn. **84**, 1–2 (2016)
6. Gao, J., Hu, J., Tung, W.W.: Entropy measures for biological signal analyses. Nonlinear Dyn. **68**, 431–444 (2012)
7. Yan, J., Wang, Y., Ouyang, G., Yu, T., Li, Y., Sik, A., Li, X.: Analysis of electrocorticogram in epilepsy patients in terms of criticality. Nonlinear Dyn. **83**, 1909–1917 (2016)
8. Daly, D., Pedley, T.A.: Current Practice of Clinical Electroencephalography. Raven Press, New York (1990)
9. Spuler, M.: A high-speed brain-computer interface (BCI) using dry EEG electrodes. PLoS ONE **12**(2), 1–12 (2017)
10. Bowsher, K., Civillico, E., Coburn, J., Collinger, J., Contreras-Vidal, J., Denison, T., Donoghue, J., French, J., Getzoff, N., Hochberg, L., et al.: Brain-computer interface devices for patients with paralysis and amputation: a meeting report. J. Neural Eng. **13**(2), 023001 (2016)
11. Zhang, Y., Yin, E., Li, F., Zhang, Y., Tanaka, T., Zhao, Q., Cui, Y., Xu, P., Yao, D., Guo, D.: Two-stage frequency recognition method based on correlated component analysis for SSVEP-based BCI. IEEE Trans. Neural Syst. Rehabil. Eng. **26**(7), 1314–1323 (2018)
12. Zhang, Y., Guo, D., Li, F., Yin, E., Zhang, Y., Li, P., Zhao, Q., Tanaka, T., Yao, D., Xu, P.: Correlated component analysis for enhancing the performance of SSVEP-based brain-computer interface. IEEE Trans. Neural Syst. Rehabil. Eng. **26**(5), 948–956 (2018)
13. Hochberg, L.R., Serruya, M.D., Friehs, G.M., Mukand, J.A., Saleh, M., Caplan, A.H., Branner, A., Chen, D., Penn, R.D., Donoghue, J.P.: Neuronal ensemble control of prosthetic devices by a human with tetraplegia. Nature **442**, 164–171 (2006)
14. Chaudhary, U., Birbaumer, N., Ramos-Murguialday, A.: Brain-computer interfaces for communication and rehabilitation. Nat. Rev. Neurol. **12**, 513–525 (2016)
15. De Nunzio, A.M., Dosen, S., Lemling, S., Markovic, M., Schweisfurth, M.A., Ge, N., Graimann, B., Falla, D., Farina, D.: Tactile feedback is an effective instrument for the training of grasping with a prosthesis at low- and medium-force levels. Exp. Brain Res. **235**(8), 2547–2559 (2017)
16. Gonzalez, J., Soma, H., Sekine, M., Yu, W.: Psychophysiological assessment of a prosthetic hand sensory feedback system based on an auditory display: a preliminary study. J. NeuroEng. Rehabil. **9**(33), 1–14 (2012)
17. Raspopovic, S., Capogrosso, M., Petrini, F.M., Bonizzato, M., Rigosa, J., Di Pino, G., Carpaneto, J., Controzzi, M., Boretius, T., Fernndez, E., Granata, G., Oddo, C.M., Citi, L., Ciancio, A.L., Cipriani, C., Carrozza, M.C., Jensen, W., Guglielmelli, E., Stieglitz, T., Rossini, P.M., Micera, S.: Restoring natural sensory feedback in real-time bidirectional hand prostheses. Sci. Transl. Med. **6**, 222 (2014)
18. De Pascalis, V., Silveri, A.: Effects of feedback control on EEG alpha asymmetry during covert mental tasks. Int. J. Psychophysiol. **3**, 163–170 (1986)
19. Touron, D.R., Hertzog, C.: Accuracy and speed feedback: global and local effects on strategy use. Exp. Aging Res. **40**, 332–356 (2014)
20. Yagasaki, K.: Chaos in a pendulum with feedback control. Nonlinear Dyn. **6**, 125–142 (1994)
21. Yagasaki, K.: A simple feedback control system: bifurcations of periodic orbits and chaos. Nonlinear Dyn. **9**, 391–417 (1996)
22. Yabuno, H.: Bifurcation control of parametrically excited duffing system by a combined linear-plus-nonlinear feedback control. Nonlinear Dyn. **12**(3), 263–274 (1997)
23. Martnez-Zrega, B.E., Pisarchik, A.N., Tsimring, L.S.: Using periodic modulation to control coexisting attractors induced by delayed feedback. Phys. Lett. A **318**, 102–111 (2003)
24. Pisarchik, A.N., Feudel, U.: Control of multistability. Phys. Rep. **540**, 167–218 (2014)
25. Zhu, W.Q., Ying, Z.G., Soong, T.T.: An optimal nonlinear feedback control strategy for randomly excited structural systems. Nonlinear Dyn. **24**, 31–51 (2001)
26. Masoud, Z.N., Nayfeh, A.H.: Sway reduction on container cranes using delayed feedback controller. Nonlinear Dyn. **34**, 347–358 (2003)
27. Bhoir, N., Singh, S.N.: Output feedback modular adaptive control of a nonlinear prototypical wing section. Nonlinear Dyn. **37**, 357373 (2004)
28. Sevilla-Escoboza, R., Pisarchik, A.N., Jaimes-Reategui, R., Huerta-Cuellar, G.: Selective monostability in multi-stable systems. Proc. R. Soc. Lon. A **471**(2180), 1–15 (2015)
29. Sevilla-Escoboza, R., Huerta-Cuellar, G., Jaimes-Reategui, R., Medel-Ruiz, C.I., Castaneda, C.E., Lopez-Mancilla, D., Pisarchik, A.N.: Error-feedback control of multistability. J. Franklin Inst. **354**(16), 7346–7358 (2017)
30. Maksimenko, V.A., Runnova, A.E., Zhuravlev, M.O., Nedaivozov, V., Grubov, V.V., Pchelintseva, S.V., Hramov, A.E., Pisarchik, A.N.: Visual perception affected by motivation and alertness controlled by a noninvasive brain-computer interface. PLoS ONE **12**(12), 1–20 (2017)
31. Necker, L.A.: Observations on some remarkable phenomena seen in switzerland; and an optical phenomenon which occurs on viewing of a crystal or geometrical solid. Philos. Mag. **3**, 329–343 (1832)
32. Kornmeier, J., Pfaffle, M., Bach, M.: Necker cube: stimulus-related (low-level) and percept-related (high-level) EEG signatures early in occipital cortex. J. Vis. **11**(9), 12 (2011)
33. Mathes, B., Strber, D., Stadler, M.A., Basar-Eroglu, C.: Voluntary control of necker cube reversals modulates the EEG delta-and gamma-band response. Neurosci. Lett. **402**(1), 145–149 (2006)
34. Pisarchik, A.N., Jaimes-Reategui, R., Magalln-Garcia, C.D.A., Castillo-Morales, C.O.: Critical slowing down and noise-induced intermittency in bistable perception: bifurcation analysis. Biol. Cyber. **108**(4), 397–404 (2014)

35. Pisarchik, A.N., Bashkirtseva, I.A., Ryashko, L.: Controlling bistability in a stochastic perception model. Eur. Phys. J. Spec. Top. **224**(8), 1477–1484 (2015)
36. Bashkirtseva, I.A., Ryashko, L.: Stochastic sensitivity of a bistable energy model for visual perception. Indian J. Phys. **91**(1), 57–62 (2017)
37. Wang, M., Arteaga, D., He, B.J.: Brain mechanisms for simple perception and bistable perception. Proc. Nat. Acad. Sci. **110**(35), E3350–E3359 (2013)
38. Mulckhuyse, M., Kelley, T.A., Theeuwes, J., Walsh, V., Lavie, N.: Enhanced visual perception with occipital transcranial magnetic stimulation. Eur. J. Neurosci. **34**(8), 1320–1325 (2011)
39. Gleiss, S., Kayser, C.: Acoustic noise improves visual perception and modulates occipital oscillatory states. J. Cogn. Neurosci. **26**(4), 699–711 (2014)
40. Laufs, H., Holt, J.L., Elfont, R., Krams, M., Paul, J.S., Krakow, K., Kleinschmidt, A.: Where the BOLD signal goes when alpha EEG leaves. Neuroimage **31**(4), 1408–1418 (2006)
41. Niedermeyer, E., Lopes da Silva, F.H. (eds.): Electroencephalography. Basic Principles, Clinical Applications, and Related Fields, 5th edn. Lippincott, Williams& Wilkins, Philadelphia (2005)
42. Hramov, A.E., Maksimenko, V.A., Pchelintseva, S.V., Runnova, A.E., Grubov, V.V., Musatov, V.Y., Zhuravlev, M.O., Koronovskii, A.A., Pisarchik, A.N.: Classifying the perceptual interpretations of a bistable image using EEG and artificial neural networks. Front. Neurosci. **11**, 674 (2017)
43. Leopold, D.A., Wilke, M., Maier, A., Logothetis, N.K.: Stable perception of visually ambiguous patterns. Nat. Neurosci. **5**(6), 605–609 (2002)
44. Kornmeier, J., Ehn, W., Bigalke, H., Bach, M.: Discontinuous presentation of ambiguous figures: How interstimulus-interval durations affect reversal dynamics and ERPs. Psychophysiol. **44**(4), 552–560 (2007)
45. Pavlov, A.N., Hramov, A.E., Koronovskii, A.A., Sitnikova, Y.E., Makarov, V.A., Ovchinnikov, A.A.: Wavelet analysis in neurodynamics. Physics-Uspekhi **55**(9), 845–875 (2012)
46. Hramov, A.E., Koronovskii, A.A., Makarov, V.A., Pavlov, A.N., Sitnikova, E.: Wavelets in Neuroscience. Springer, Berlin (2015)
47. Ogden, T.: Essential Wavelets for Statistical Applications and Data Analysis. Springer, New York (2012)
48. Sitnikova, E., Hramov, A.E., Grubov, V., Koronovsky, A.A.: Time-frequency characteristics and dynamics of sleep spindles in WAG/Rij rats with absence epilepsy. Brain Res. **1543**, 290–299 (2014)
49. Maksimenko, V.A., Runnova, A.E., Frolov, N.S., Makarov, V.V., Nedaivozov, V.O., Koronovskii, A.A., Pisarchik, A.N., Hramov, A.E.: Multiscale neural connectivity during human sensory processing in the brain. Phys. Rev. E **97**, 052405 (2018)
50. Michalareas, G., Vezoli, J., van Pelt, S., Schoffelen, J.M., Kennedy, H., Fries, P.: Alpha–beta and gamma rhythms subserve feedback and feedforward influences among human visual cortical areas. Neuron **384**, 384–397 (2016)
51. Buffalo, E.A., Fries, P., Landman, R., Buschman, T.J., Desimone, R.: Laminar differences in gamma and alpha coherence in the ventral stream. Proc. Natl. Acad. Sci. United States of Am. **108**(11), 262–267 (2011)
52. Roy, R.N., Charbonnier, S., Campagne, A., Bonnet, S.: Efficient mental workload estimation using task-independent EEG features. J. Neural Eng. **13**, 026019 (2016)
53. Chaudhuri, A., Behan, P.O.: Fatigue and basal ganglia. J. Neurolog. Sci. **179**(1–2), 34–42 (2000)
54. Mizuno, K., Tanaka, M., Yamaguti, K., Kajimoto, O., Kuratsune, H., Watanabe, Y.: Mental fatigue caused by prolonged cognitive load associated with sympathetic hyperactivity. Behav. Brain Fun. **7**(1), 17 (2011)
55. Bonnefond, A., Doignon-Camus, N., Touzalin-Chretien, P., Dufour, A.: Vigilance and intrinsic maintenance of alert state: an ERP study. Behav. Brain Res. **211**(2), 185–190 (2010)
56. Boksem, M.A., Meijman, T.F., Lorist, M.M.: Effects of mental fatigue on attention: an ERP study. Cogn. Brain Res. **25**(1), 107–116 (2005)
57. Kato, Y., Endo, H., Kizuka, T.: Mental fatigue and impaired response processes: event-related brain potentials in a go/nogo task. Int. J. Psychophysiol. **72**(2), 204–211 (2009)
58. Faber, L.G., Maurits, N.M., Lorist, M.M.: Mental fatigue affects visual selective attention. PloS ONE **7**(10), e48,073 (2012)
59. Guo, Z., Chen, R., Zhang, K., Pan, Y., Wu, J.: The impairing effect of mental fatigue on visual sustained attention under monotonous multi-object visual attention task in long durations: an event-related potential based study. PloS ONE **11**(9), e0163360 (2016)
60. Klimesch, W.: Eeg alpha and theta oscillations reflect cognitive and memory performance: a review and analysis. Brain Res. Rev. **29**(2–3), 169–195 (1999)
61. Tanaka, M., Shigihara, Y., Ishii, A., Funakura, M., Kanai, E., Watanabe, Y.: Effect of mental fatigue on the central nervous system: an electroencephalography study. Behav. Brain Funct. **8**(1), 48 (2012)
62. Zhao, C., Zhao, M., Liu, J., Zheng, C.: Electroencephalogram and electrocardiograph assessment of mental fatigue in a driving simulator. Accid. Anal. Prev. **45**, 83–90 (2012)
63. Baars, B.J.: In the theatre of consciousness. global workspace theory, a rigorous scientific theory of consciousness. J. Conscious. Stud. **4**(4), 292–309 (1997)
64. Dehaene, S., Kerszberg, M., Changeux, J.P.: A neuronal model of a global workspace in effortful cognitive tasks. Proc. Natl. Acad. Sci. **95**(24), 14529–14534 (1998)
65. Finc, K., Bonna, K., Lewandowska, M., Wolak, T., Nikadon, J., Dreszer, J., Duch, W., Kühn, S.: Transition of the functional brain network related to increasing cognitive demands. Hum. Brain Mapp. **38**(7), 3659–3674 (2017)
66. Guo, D., Guo, F., Zhang, Y., Li, F., Xia, Y., Xu, P., Yao, D.: Periodic visual stimulation induces resting-state brain network reconfiguration. Front. Comput. Neurosci. **12**, 21 (2018)
67. Fox, M.D., Snyder, A.Z., Vincent, J.L., Corbetta, M., Van Essen, D.C., Raichle, M.E.: The human brain is intrinsically organized into dynamic, anticorrelated functional networks. Proc. Natl. Acad. Sci. **102**(27), 9673–9678 (2005)
68. Corbetta, M., Shulman, G.L.: Control of goal-directed and stimulus-driven attention in the brain. Nat. Rev. Neurosci. **3**(3), 201 (2002)
69. Wojciulik, E., Kanwisher, N.: The generality of parietal involvement in visual attention. Neuron **23**(4), 747–764 (1999)

70. Mckiernan, K.A., Kaufman, J.N., Kucera-Thompson, J., Binder, J.R.: A parametric manipulation of factors affecting task-induced deactivation in functional neuroimaging. J. Cogn. Neurosci. **15**(3), 394–408 (2003)
71. Marois, R., Ivanoff, J.: Capacity limits of information processing in the brain. Trends in Cogn. Sci. **9**(6), 296–305 (2005)
72. Vogel, E.K., Machizawa, M.G.: Neural activity predicts individual differences in visual working memory capacity. Nature **428**(6984), 748 (2004)
73. Todd, J.J., Marois, R.: Capacity limit of visual short-term memory in human posterior parietal cortex. Nature **428**(6984), 751 (2004)
74. Gross, J., Schmitz, F., Schnitzler, I., Kessler, K., Shapiro, K., Hommel, B., Schnitzler, A.: Modulation of long-range neural synchrony reflects temporal limitations of visual attention in humans. Proc. Natl. Acad. Sci. **101**(35), 13050–13055 (2004)
75. Marois, R., Chun, M.M., Gore, J.C.: Neural correlates of the attentional blink. Neuron **28**(1), 299–308 (2000)
76. Taya, F., Sun, Y., Babiloni, F., Thakor, N., Bezerianos, A.: Brain enhancement through cognitive training: a new insight from brain connectome. Front. Sys. Neurosci. **9**, 44 (2015)
77. Klingberg, T.: Training and plasticity of working memory. Trends Cogn. Sci. **14**(7), 317–324 (2010)
78. Jolles, D., Crone, E.A.: Training the developing brain: a neurocognitive perspective. Fron. Hum. Neurosci. **6**, 76 (2012)
79. Hempel, A., Giesel, F.L., Garcia Caraballo, N.M., Amann, M., Meyer, H., Wüstenberg, T., Essig, M., Schröder, J.: Plasticity of cortical activation related to working memory during training. Am. J. Psychiatry **161**(4), 745–747 (2004)
80. Olesen, P.J., Westerberg, H., Klingberg, T.: Increased prefrontal and parietal activity after training of working memory. Nat. Neurosci. **7**(1), 75 (2004)
81. Draganski, B., May, A.: Training-induced structural changes in the adult human brain. Behav. Brain Res. **192**(1), 137–142 (2008)
82. Driemeyer, J., Boyke, J., Gaser, C., Büchel, C., May, A.: Changes in gray matter induced by learning-revisited. PloS One **3**(7), e2669 (2008)
83. Scholz, J., Klein, M.C., Behrens, T.E., Johansen-Berg, H.: Training induces changes in white-matter architecture. Nat. Neurosci. **12**(11), 1370 (2009)
84. Wolf, D., Fischer, F.U., Fesenbeckh, J., Yakushev, I., Lelieveld, I.M., Scheurich, A., Schermuly, I., Zschutschke, L., Fellgiebel, A.: Structural integrity of the corpus callosum predicts long-term transfer of fluid intelligence-related training gains in normal aging. Hum. Brain Mapp. **35**(1), 309–318 (2014)
85. Maksimenko, V.A., Lu'uttjohann, A., Makarov, V.V., Goremyko, M.V., Koronovskii, A.A., Nedaivozov, V., Runnova, A.E., van Luijtelaar, G., Hramov, A.E., Boccaletti, S.: Macroscopic and microscopic spectral properties of brain networks during local and global synchronization. Phys. Rev. E **96**, 012316 (2017)
86. Rubchinsky, L.L., Park, C., Worth, R.M.: Intermittent neural synchronization in parkinsons disease. Nonlinear Dyn. **68**, 329346 (2012)
87. Lehnertz, K.: Epilepsy: Extreme Events in the Human Brain. Springer, Berlin, Heidelberg (2006)
88. Pisarchik, A.N., Grubov, V.V., Maksimenko, V.A., Lttjohann, A., Frolov, N.S., Marqués-Pascual, C., Gonzalez-Nieto, D., Khramova, M., Hramov, A.E.: Extreme events in epileptic EEG of rodents after ischemic stroke. Eur. Phys. J. Spec. Top. **227**(7–9), 3921–932 (2018)
89. Kinreich, S., Djalovski, A., Kraus, L., Louzoun, Y., Feldman, R.: Brain-to-brain synchrony during naturalistic social interactions. Sci. Rep. **7**(1), 17060 (2017)